琉球大学学術リポジトリ

水平管群を流下する液膜表面波の生成とガス吸収促進の機構解明

メタデータ	言語:
	出版者: 野底武浩
	公開日: 2009-06-29
	キーワード (Ja): 表面波, ガス吸収, 流下液膜, 拡散, 水平管, 物質移動, 物質伝達
	キーワード (En): Mass transfer, Liquid film, Mass diffusion, Gas absorption, Horizontal tubes, Surface wave
	作成者: 野底, 武浩, 儀間, 悟, 宮良, 明男, Nosoko, Takehiro, Gima, Satoru, Miyara, Akio
	メールアドレス:
	所属:
URL	http://hdl.handle.net/20.500.12000/11007

第2章

鉛直面を流下する液膜の流動と
ガス吸収促進機構の解明

2.1 Wave-augmented mass transfer in a liquid film falling inside a vertical tube

Abstract

Uniformly distributed water films were formed inside vertical tubes, and partial disintegrations of hump-like surface waves (or large waves) into clusters of dimples were observed on the films at the Reynolds number $Re\sim40$ and larger, associated with marked deceleration of mass-transfer augmentation. In about 1 m or taller films with the uniform distribution, two empirical correlations between the Sherwood number Sh and Re at the ranges of $Re=20$–40 and 40–400 were constructed. The transition to turbulent flow occurs in the films with decelerating inlet flow at the range of $Re=400$–700 where Sh sharply rises, suggesting that the laminar developing entry region rapidly shortens to nearly disappear, though the region had been observed only in film flow measurements. Periodic perturbations imposed on the inlet flow trigger tall humps close to the inlet, causing the laminar developing region to vanish and the critical Re to reduce from 400 to about 300. Waves covering a whole film of 0.4–1.0 m height increase in Sh up to 2.2–2.7 times the theoretical prediction for a smooth film at the laminar-flow range. The amount of increase is larger in a taller film. The decrease in Sh due to the tube inclination from the vertical is more serious for a taller film with laminar flow, and a 0.2° inclination causes a 5% decrease in a 0.7 m tall film.

Keywords: Falling film; Surface wave; Mass transfer; Flow transition; Turbulent flow; Laminar entry region

Nomenclature

C	dissolved oxygen concentration, g/m^3
D	mass diffusivity, m^2/s
f	frequency of periodic inlet perturbation, 1/s
g	gravitational acceleration, m/s^2
k_L	mean mass transfer coefficient, m/s
L_{sm}	length of smooth entry pass, m
L_f	film height, m
Q	volumetric flow rate, m^3/s
R	inner radius of tube, m
Re	Reynolds number, $Q/(2\pi R v)$
Sc	Schmidt number, v/D
Sh	Sherwood number, $(k_L\ \delta)/D$
x	downstream distance from the film inlet, m

Greek symbols

δ mean film thickness, m

ν kinematic viscosity, m²/s

θ tube inclination from vertical, deg.

Subscripts

fc   forced wave

in   film entry

N   Nusselt film

nt   naturally formed wave

out   film exit

s   saturated

1. Introduction

Falling liquid films are widely utilized in industry for interfacial heat/mass transfer processes in gas absorbers, chemical reactors, evaporators, condensers, cooling towers, etc. Wave-induced convections are most intense at or near the film surface, and thus they drastically augment the mass transfer from the surface into the bulk of film and vice versa; otherwise the mass transfer rate is very small due to the low molecular diffusion. Several researchers measured the mean mass transfer coefficient k_L in films falling down vertical walls at various flow rates as reviewed by Alekseenko et al. [1], Roberts & Chang [2], Bakopoulos [3], Hikita et al. [4] and Kamei & Oishi [5]. These measurements show that the mean mass transfer coefficient k_L rapidly increases at small *Re*, after which the rate of increase suddenly drops at a certain *Re* and then continue to increase slowly until the turbulent-flow range of *Re* is reached whereby the coefficient starts to sharply increase again. The critical Reynolds numbers seem to be in 40–75 and 300–400 for the first and second transitions, respectively, though the measurements scatter widely. In the laminar flow range surface waves may augment the coefficient k_L of 0.3–0.65 m and 1.1–2.5 m tall films up to 2–3 and 2.5–5.5 times the prediction for a flat film, respectively [2]. For practical use, Bakopoulos [3] constructed empirical correlations of the Sherwood number *Sh* as a function of *Re* at the three *Re* ranges for water films. He selected the measurements of Kamei & Oishi [5], Hikita et al. [4], Lamourelle & Sandall [6] and Emmert & Pigford [7] where most of the data had been determined in 1 m or taller films, so that his correlations can neglect the effect of the film height or the smooth entry pass. Waves appear at some downstream distance on the entry smooth surface, and the length of the smooth entry pass increases with *Re* up to about 0.3 m [8].

The dynamics of surface waves varies with both the flow rate and the downstream distance x

[9–15]. Waves appear on the smooth surface and soon coalesce to develop into teardrop-shaped tall waves (or humps) traveling on a thin substrate at high speeds [16]. The consequent humps (often referred to as 'large waves' [17]) intermittently coalesce to further develop into taller humps with large separations [18–20]. Such process of integrating waves into lesser numbers of taller humps is observed at wide Re ranges of both laminar and turbulent flow, and the wave integration process seems to be rapid to distances of about 0.5 m from the film inlet and then become slow further downstream. Takahama & Kato [13] measured film thickness variations at various downstream distances and showed that the amplitude of humps and the standard deviation of film-thickness variation rapidly increase in about 0.5 m long entry zone. Humps out of the entry zone have a nearly constant dimensionless speed of about 1.3 with respect to the mean velocity in the film, and gradually increase the mean separation between humps. Such slow integration process continues to $x\sim2.5$ m or further downstream at $Re\sim170$ and larger, associated with a gradual increase in the standard deviation of film thickness [15]. The wave dynamics might reach the final saturation at $x\sim6$ m or further downstream [12].

The humps undergo not only the wave integration but also partial disintegration. Recently Park & Nosoko [16] revealed that humps disintegrate into several horseshoe-shaped humps at $Re\sim40$ or larger, causing the first transition of the mass transfer, and the partial disintegration become more intense at larger Re associated with the marked deceleration of the mass transfer augmentation.

For the film flow, the structure of turbulent flow and the transition to turbulent flow have not been fully understood in spite of numerous studies on falling films. The film flow is *wavy-laminar* in the laminar-flow range, and the transition to turbulent flow seems to occur in a manner different from that observed in wall boundary shear layers. Karimi & Kawaji [21,22] detected *localized* turbulent flow under waves with large fluctuations of film-surface height. From the breaks in curves of the local mean film thickness vs. Re, Takahama & Kato [13] detected the transition to turbulent flow, and derived the conclusion that a film has a wavy-laminar entry region preceding to the transition to turbulent flow and this laminar developing entry region gradually retracts upstream from $x\sim1.3$ m to ~0.9 m with Re increasing from 370 to 750 and then rapidly diminishes to be close to the inlet at $Re\sim800$ or larger. Brauer's [11], Feind's [23] and Wilke's [24] experiments may support Takahama & Kato's findings, and suggest the transition range from $Re\sim400$ to 800; At this Re range, the wave peak height become constant [11], the mean heat transfer coefficient from tube wall to film has the largest slope of the coefficient–Re curve on log–log graph [24], and the mean film thickness curves have breaks within the Re range for liquids of various viscosities and surface tensions. One may expect that such behavior of the laminar developing entry region brings about drastic changes in the mass transfer between the surface and the bulk at the transition Re range.

In the present work, we determined the mean mass transfer coefficient k_L for films discharged

uniformly through the newly designed feeding device (see Fig. 1) that greatly improves the uniform distribution of liquid along a tube inner circumference. A slight variation of the distribution causes a serious reduction in the mass transfer rate. The new design is an updated version of the 'undulated annular distributor' designed by Brauer [25], in which liquid is discharged into a film through several channels arranged along the circumference. Though in most of engineering applications and experimental studies, falling films have been formed on tube walls by liquid flowing over a weir or through ring slots [3,26], both methods have serious difficulties in obtaining uniform distribution, especially at low flow rates. According to Bakopoulos [3] and our preliminary experiments, diminutive variations in the slot width and in liquid velocity entering the slot may ruin the uniform distribution, and for the overflowing, diminutive manufacturing defects of the tube top edge, flow disturbances in liquid pool around the tube edge and imperfection of vertical tube alignment.

With the uniformly distributed films, we explored the mass transfer in the transition range from the wavy-laminar to turbulent flow, as well as the effect of the smooth entry pass on the mass transfer at the laminar-flow range, by imposing perturbations of a low constant frequency on the inlet film flow. Such inlet forcings may greatly shorten both the laminar developing entry region preceding the transition to turbulent flow and the smooth entry pass preceding the wavy-laminar flow. The initial evolution of the wave is extremely sensitive to disturbances included in the inlet flow, and the *naturally* formed waves, which have been investigated by many researchers, are noise-driven and have frequencies within a narrow band at their inception [18,27]. Then the waves (or humps) increase the separations through coalescence events as they travel downstream. When the inlet forcings are adequately larger in amplitude than the noise included in the inlet flow, waves at the corresponding low frequency appear close to the inlet, and then directly grow into tall humps with large separations. Comparisons in the mass transfer between the forced waves and the natural waves may allow one to determine the variation of the laminar developing entry region in the transition range of *Re*, as well as the effect of the smooth entry pass on the mass transfer at the laminar-flow range. Furthermore, we examined the effect of the tube inclination θ from the vertical, which may be important when installing equipment in practical applications. Liquid uniformly discharged at the inlet may gradually accumulate as it flows downstream inside a slightly inclined tube, causing a reduction of the mass transfer rate. This tube inclination effect can be determined with uniform distribution.

2. Experimental apparatus and procedure

Tap water flows from a head tank through a silicone tube into a two-story holding compartment at the top of glass tube, and then the water is uniformly distributed through 17 capillary tubes arranged along the 9.6 mm inner tube wall to form a film (Fig. 1). Oxygen-rich
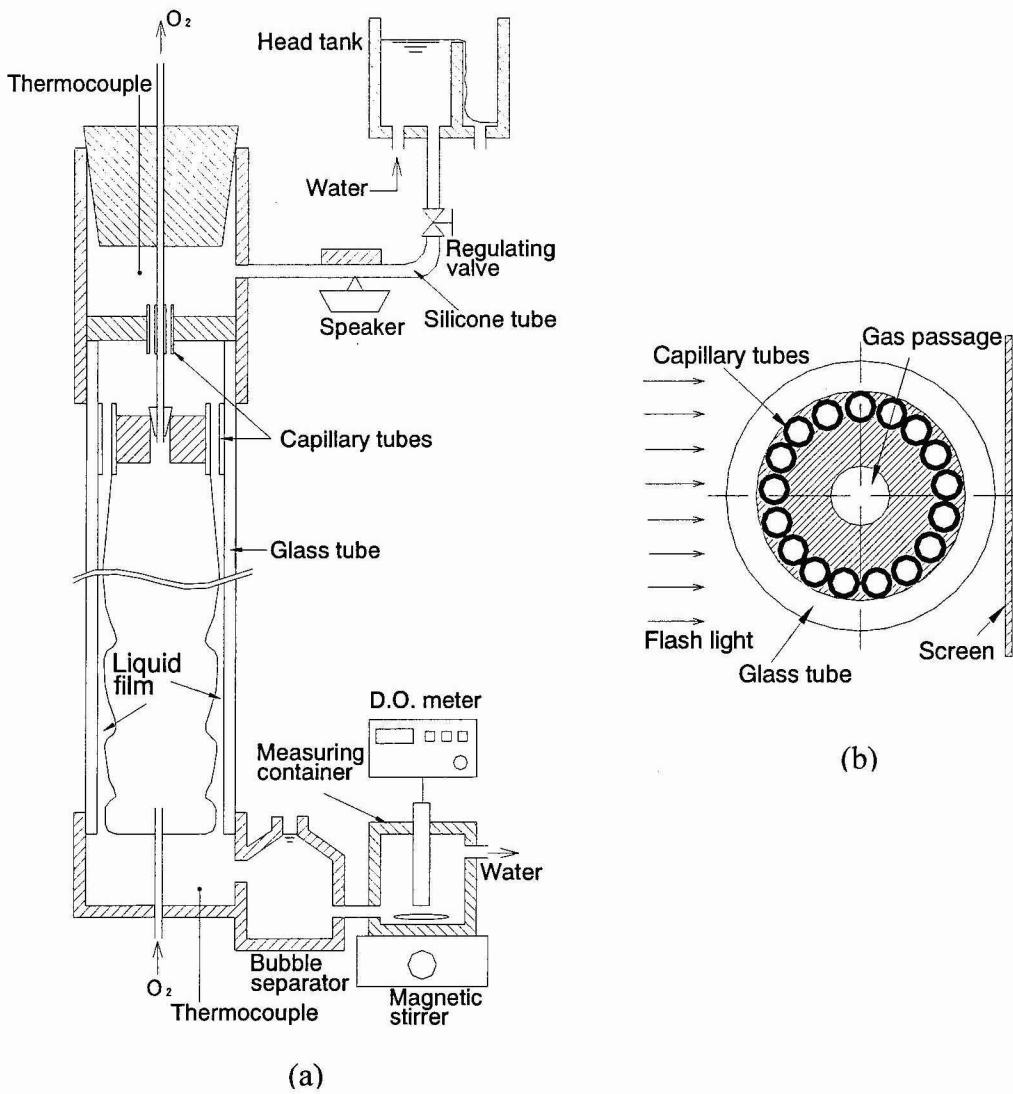
Fig.1 Experimental apparatus: (a) Flow diagram of water and oxygen gas and (b) cross-section of distributor consisting of capillary tubes, and arrangement of screen, glass tube and light rays.

water flows from the pool at the bottom of the tube through a bubble separator into a measuring container where the dissolved oxygen concentration C_{out} is measured with a galvanic cell within 1% error. Oxygen gas flows upwards through the tube core space and its flow rate is so low that both the pressure rise inside the tube as a result of the gas flow and the effect of the gas flow on the wave dynamics are negligible. A thin plate fixed to a speaker cone vibrates the silicone tube to impose periodic perturbations on the water flow. Power input into the speaker is adjusted to trigger large waves (or humps) to develop shortly downstream of the film inlet. A holder of the glass tube is fixed to a steel pole standing on a mechanical stage, which can change the tube inclination θ with 0.08° accuracy.

The capillary tubes are 15 mm long and 1.0 mm inner diameter (Fig. 1-b), and differences in flow rate through each tube are very small (within ±2%). Jets from the tubes merge at the tube exits to form a film, and thus the inlet film flow includes transverse disturbances of a 1.4 mm wavelength, i.e. the interval between tubes. This transverse wavelength is much shorter than the most unstable wavelength of about 2 cm found by Park & Nosoko [16]. The average velocity in each tube exceeds the average velocity in the smooth entry to the film (equal to the average velocity in Nusselt film) at $Re\sim280$ or larger, showing that the flow decelerates in the entry at $Re\sim280$ or larger. At large Re, the film drags along bubbles into the water pool at the bottom. The water flow from the pool brings about a circulation flow inside the bubble separator for the bubbles to accumulate in the center and float up to the water surface.

The water temperature was measured by the calibrated T-type thermocouples at the top and bottom of the tube within a ±0.1 K error, and the average of both readings, i.e. the film temperature, was 15–24 °C for the mass transfer measurements. The mass flow rate of water was measured at the exit of the container within a ±0.5% error. The oxygen concentration in tap water was measured before and after the experimental runs in a day, and the average of these two was assumed to be the inlet concentration C_{in}, though the differences between the two were less than 1% for most of the measurements.

Flashlight from a stroboscope passes through the glass tube and projects the shadows of the film on the screen (Fig. 1-b). The shadow image is captured by a camera synchronized with the stroboscope. The flashlight passes through the annular film, and therefore two shadow images of front and back parts of the tube inner wall are projected, overlapping on the screen and the tube curvature distorts wave shadows. These may bring some difficulty when one observes the shadow images.

We employ the Reynolds number Re, the Schmidt number Sc and the Sherwood number Sh defined as,

$$Re = \frac{Q}{(2\pi R \nu)}, \qquad Sc = \frac{\nu}{D}, \qquad Sh = \frac{k_L \delta}{D} \qquad (1)–(3)$$

where the mean film thickness δ is calculated from one of the following correlations,

$$\delta = \left(\frac{3v^2 Re}{g}\right)^{1/3} \quad \text{at } Re < 400, \qquad \delta = 0.302\left(\frac{3v^2}{g}\right)^{1/3} Re^{8/15} \qquad \text{at } Re > 400 \qquad (4), (5)$$

The first equation for δ is applicable to the fully developed flat film (referred to as Nusselt film) and *wavy-laminar* films, and the second, to turbulent-flow films [11].

The mean mass transfer coefficient k_L is calculated from

$$k_L = \frac{Q}{2\pi(R-\delta)L_f}\ln\frac{C_s - C_{in}}{C_s - C_{out}} \qquad (6)$$

The saturated concentration C_s was calculated from Truesdale et al.'s [28] correlation with the film temperature and the partial pressure of oxygen at the film surface. The partial pressure was assumed to be the difference between the ambient pressure and the saturate pressure of water at the film temperature. An error in k_L or Sh arising from the measurements of C, Q and L_f is small, and diminutive imperfection of uniform distribution and excess absorption from bubbles pulled into the water dominate the overall error in Sh, which is roughly estimated to be $\pm 4\%$ at the laminar-flow range of Re from the scattering of the measurements and others. At the turbulent-flow range, the bubble separator could not remove the bubbles pulled into the water completely. Thus the measurements of Sh have positive deviations at the turbulent-flow range, and this is discussed in the proceeding section. The error in Re is found to be $\pm 1\%$ or less. The diffusivity D was calculated from Stokes-Einstein equation (refer to [16, 30]), and the Schmidt number Sc was estimated to be 644–403 at the present working temperature of $T = 15$–24 °C.

3. Results and discussion

3.1. Wave dynamics

Teardrop-like waves (or humps) have deep valleys in their fronts and the front valleys form distinctive dark strips on the screen, which may represent their wavefronts [16,29,30]. Shadow images of surface waves are shown in Figs. 2 and 3 where several dark strips representing the wavefronts are marked by triangles with 'A' among many dark strips of wavefronts. At low Re, small waves appear on the smooth entry surface and then rapidly develop into teardrop-like tall humps (see Fig. 2-a for $Re = 20.4$). Soon the humps coalesce to develop into taller humps (Fig. 2-a for humps with longer separations at $x \sim 20$–30 cm in the shadow image of $Re = 20.4$), and then hump-coalescence events intermittently occur to generate further taller humps with much longer separations (Fig. 2-a for humps at $x > 30$ cm in the shadow image of $Re = 20.4$). Humps increase the wavefront distortion and partially disintegrate into dimples at $Re \sim 40$ or larger (Fig. 2-a for $Re = 89$) while the disintegration hardly occurs at smaller Re. One may identify such partial hump disintegrations from the resulting clusters of dimples (several clusters are marked by 'B' triangles
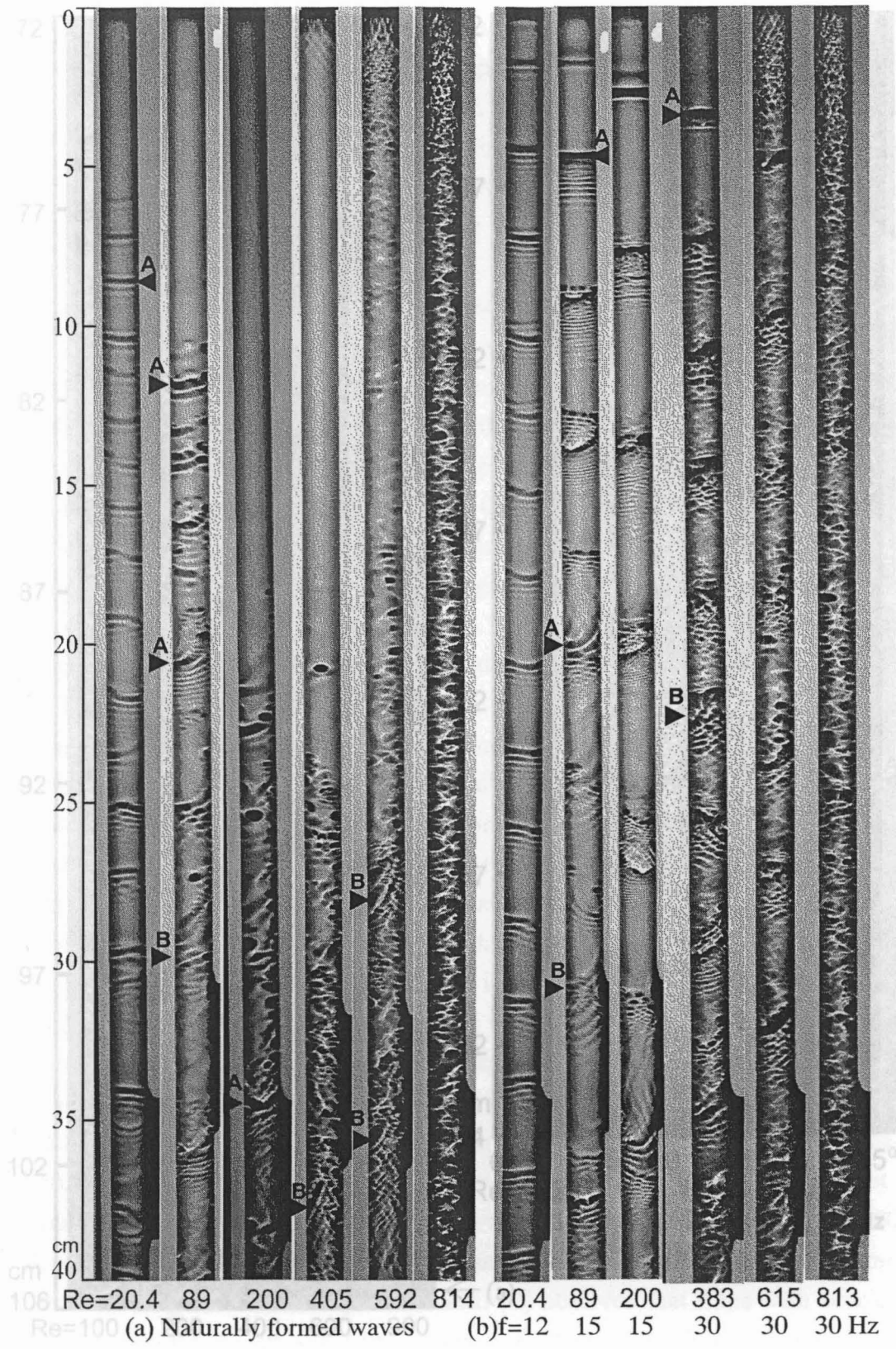
Fig. 2 Shadow images of smooth entry pass, humps and dimples at upstream region on a film at various *Re*; (a) Naturally formed humps and dimples and (b) forced humps and their partial disintegration into dimples. Dark strips and spots represent hump wavefronts and dimples, respectively, and some humps are marked by triangles with A. At high *Re*, clusters of dimples may represents humps, and some of them are marked by triangles with B.
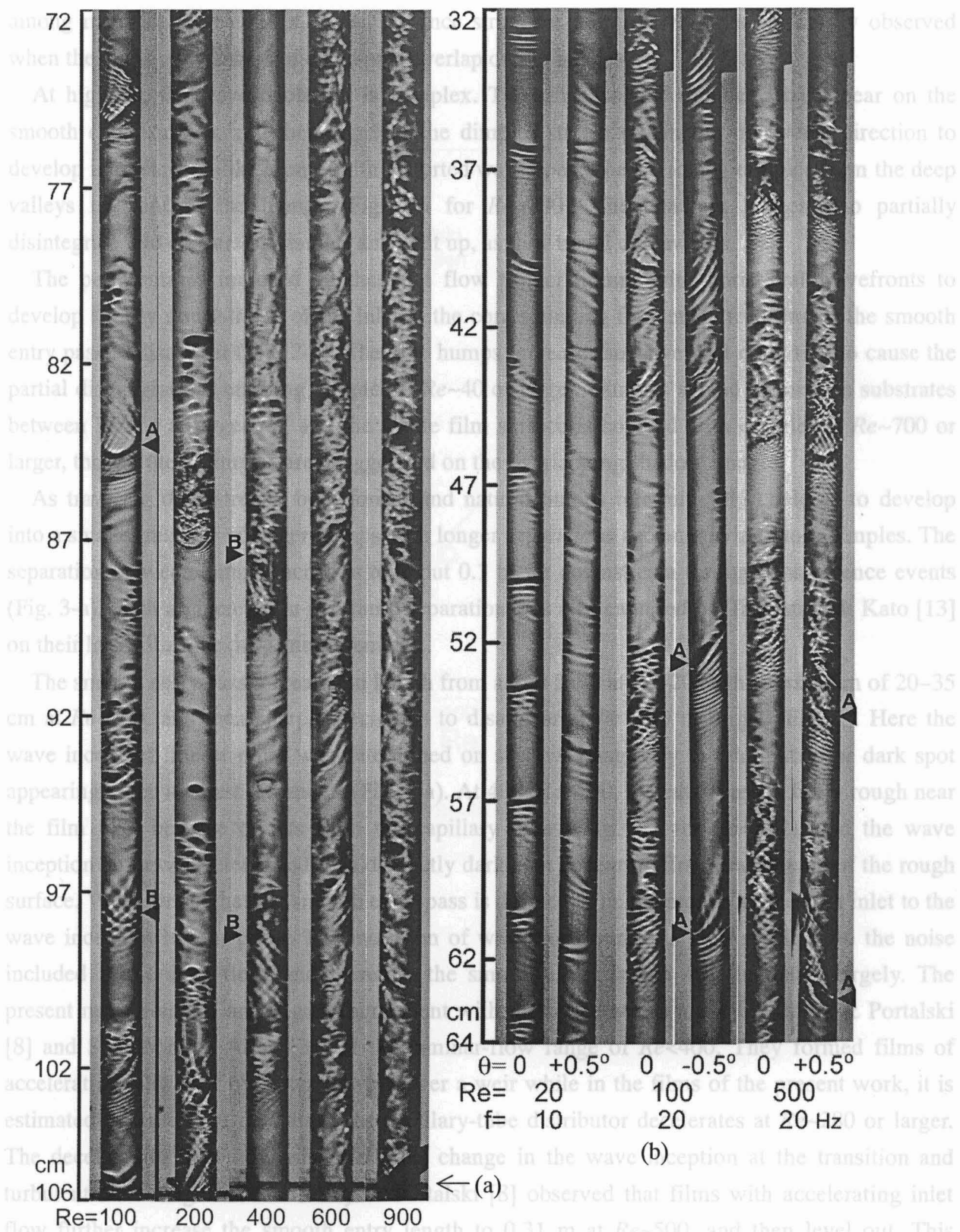
Fig. 3 Shadow images of humps and dimples at downstream and midstream regions:
(a) Naturally formed humps on a vertical film at x=0.72–1.06 m and (b) forced humps
on a vertical or inclined film at x=0.32–0.64 m.

among many clusters in Figs. 2 and 3) since strips for hump wavefronts are hardly observed when the strips and clusters of dark spots overlap on the images.

At high Re, the wave evolution is complex. Typically, isolated dimples first appear on the smooth entry surface, and then some of the dimples stretch out in the transverse direction to develop into teardrop-like humps with distorted wavefronts: the stretching dimples form the deep valleys in front of the humps (Fig. 2-a for Re=200). The resultant humps also partially disintegrate into clusters of dimples and split up, as they travel downwards.

The perturbations imposed on the inlet flow trigger humps with horizontal wavefronts to develop shortly downstream of the inlet at the corresponding frequency, resulting in the smooth entry pass to disappear (Fig. 2-b). Then the humps increase the wavefront distortion to cause the partial disintegrations emitting dimples at Re~40 or larger. Dimples spread on smooth substrates between humps at larger Re, and the whole film surface is covered with dimples at Re~700 or larger, though these dimples are exaggerated on the overlapping shadow images.

As traveling downstream, both forced and natural humps intermittently coalesce to develop into a smaller number of larger humps with longer separations accompanying more dimples. The separation between humps increases to about 0.1 m far downstream through coalescence events (Fig. 3-a). Such an increase in the hump separation was also captured by Takahama & Kato [13] on their local film-thickness measurements.

The smooth entry pass increases in length from about 5 cm at Re~20 to the maximum of 20–35 cm at Re~400, and then sharply decreases to disappear at Re~700 or larger (Fig. 4). Here the wave inception line or point was determined on shadow images by the dark strip or dark spot appearing at the shortest distance x (Fig. 2-a). At 400<Re<700, the entry pass is fairly rough near the film inlet because of jets from the capillary tubes (Fig. 2-a for Re=592), and the wave inception point was determined by a distinctly dark spot appearing first downstream of the rough surface. We assumed that the smooth entry pass is defined to be the area from the film inlet to the wave inception line or point. The inception of waves or dimples is very sensitive to the noise included in the inlet flow, and therefore the smooth entry length L_{sm} fluctuates largely. The present measurements are in good agreement with the observations made by Tailby & Portalski [8] and Stainthorp & Allen [31] at the laminar-flow range of Re<400. They formed films of accelerating inlet flow by water flowing over a weir while in the films of the present work, it is estimated that the inlet flow from the capillary-tube distributor decelerates at Re~280 or larger. The decelerating inlet flow causes a great change in the wave inception at the transition and turbulent-flow ranges of Re. Tailby & Portalski [8] observed that films with accelerating inlet flow further increase the smooth entry length to 0.31 m at Re~500, and then level out. This difference is discussed in relation to its effect on the mass transfer in the latter section.

At small Re, natural waves at their inception have nearly horizontal wavefronts, and forced waves also have nearly horizontal wavefronts even far downstream (Figs. 2-a and b for Re=20.4).
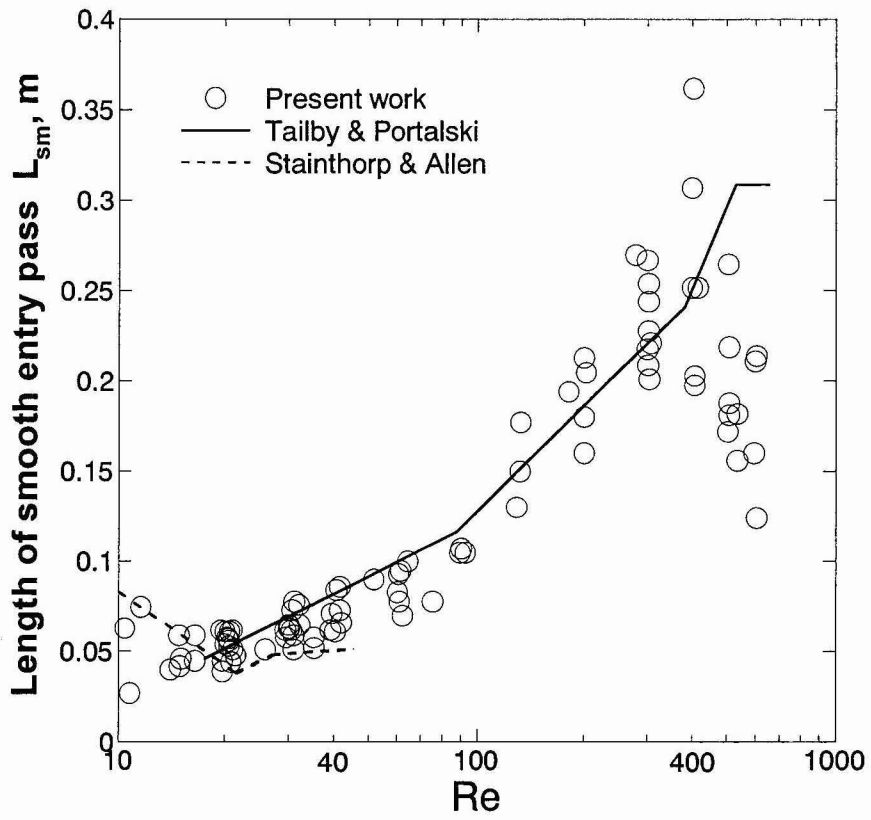
Fig. 4 Variation of length of smooth entry pass L_{sm} with Re.